Original Article

MOLECULAR METABOLISM

Tirzepatide induces a thermogenic-like amino acid signature in brown adipose tissue

Ricardo J. Samms [1,*,5], GuoFang Zhang [2,4,5], Wentao He [2], Olga Ilkayeva [2,4], Brian A. Droz [1], Steven M. Bauer [1], Cynthia Stutsman [1], Valentina Pirro [1], Kyla A. Collins [1], Ellen C. Furber [1], Tamer Coskun [1], Kyle W. Sloop [1], Joseph T. Brozinick [1], Christopher B. Newgard [2,3,4]

ABSTRACT

Objectives: Tirzepatide, a dual GIP and GLP-1 receptor agonist, delivered superior glycemic control and weight loss compared to selective GLP-1 receptor (GLP-1R) agonism in patients with type 2 diabetes (T2D). These results have fueled mechanistic studies focused on understanding how tirzepatide achieves its therapeutic efficacy. Recently, we found that treatment with tirzepatide improves insulin sensitivity in humans with T2D and obese mice in concert with a reduction in circulating levels of branched-chain amino (BCAAs) and keto (BCKAs) acids, metabolites associated with development of systemic insulin resistance (IR) and T2D. Importantly, these systemic effects were found to be coupled to increased expression of BCAA catabolic genes in thermogenic brown adipose tissue (BAT) in mice. These findings led us to hypothesize that tirzepatide may lower circulating BCAAs/BCKAs by promoting their catabolism in BAT.

Methods: To address this question, we utilized a murine model of diet-induced obesity and employed stable-isotope tracer studies in combination with metabolomic analyses in BAT and other tissues.

Results: Treatment with tirzepatide stimulated catabolism of BCAAs/BCKAs in BAT, as demonstrated by increased labeling of BCKA-derived metabolites, and increases in levels of byproducts of BCAA breakdown, including glutamate, alanine, and 3-hydroxyisobutyric acid (3-HIB). Further, chronic administration of tirzepatide increased levels of multiple amino acids in BAT that have previously been shown to be elevated in response to cold exposure. Finally, chronic treatment with tirzepatide led to a substantial increase in several TCA cycle intermediates (α-ketoglutarate, fumarate, and malate) in BAT.

Conclusions: These findings suggest that tirzepatide induces a thermogenic-like amino acid profile in BAT, an effect that may account for reduced systemic levels of BCAAs in obese IR mice.

Keywords Tirzepatide; GIPR; GLP-1R; BCAAs; BCKAs; BAT

1. INTRODUCTION

The dramatic worldwide rise in the prevalence of obesity and type 2 diabetes (T2D) over the past 50 years [1,2], coupled with a lack of optimal therapeutics, has recently fueled the discovery and development of next generation diabetes medications [3,4]. Multi-receptor agonists harnessing the activity of the glucose-dependent insulinotropic polypeptide (GIP) and glucagon-like peptide-1 (GLP-1) receptors are at the forefront of a new era of novel therapies designed for treating metabolic diseases [5]. Tirzepatide is a dual GIP and GLP-1 receptor agonist that has demonstrated improved glycemic control and superior weight loss when compared to treatment with selective GLP-1 receptor (GLP-1R) agonists in patients with T2D [6,7]. These clinical findings have prompted interest in gaining a better understanding of mechanism(s) by which tirzepatide achieves its therapeutic benefit.

An attractive feature of multi-receptor agonists is the ability to intervene at complementary regulatory pathways, an attribute that is likely important in combating the complexity of metabolic disease. Physiologically, weight loss results in an improvement in the symptoms of T2D [8], however, a major limitation of such interventions is that body weight is often regained, with parallel reversal of improvements in glycemic control [8,9]. Importantly, treatment with tirzepatide appears to deliver both weight-dependent and -independent benefits in glycemic control [5]. For example, post-hoc analyses indicate that in subjects with T2D, some of the glycemic benefits associated with tirzepatide treatment are driven by weight-independent insulin sensitization [10]. Further, tirzepatide-mediated insulin sensitization in participants with T2D is accompanied by lowering of several circulating biomarkers associated with development of systemic insulin

[1]Lilly Research Laboratories, Lilly Corporate Center, Indianapolis, IN, 46285, USA [2]Duke Molecular Physiology Institute and Sarah W. Stedman Nutrition and Metabolism Center, Duke University School of Medicine, Durham, NC, USA [3]Department of Pharmacology and Cancer Biology, Duke University School of Medicine, Durham, NC, USA [4]Department of Medicine, Division of Endocrinology and Metabolism, Duke University School of Medicine, Durham, NC, USA

[5] Ricardo J. Samms and GuoFang Zhang contributed equally to this work.

*Corresponding author. E-mail: samms_ricardo_j@lilly.com (R.J. Samms).

Received June 16, 2022 • Revision received July 12, 2022 • Accepted July 13, 2022 • Available online 31 July 2022

https://doi.org/10.1016/j.molmet.2022.101550

resistance (IR) and T2D, including circulating triglycerides, branched-chain amino acids (BCAAs), and branched-chain ketoacids (BCKAs) [11,12].

In accordance with findings in humans treated with tirzepatide, hyperinsulinemic-euglycemic clamp studies in mice with obesity-induced IR show that tirzepatide promotes insulin sensitization [13]. In obese IR mice, we observed that tirzepatide improved insulin sensitivity to a greater extent than GLP-1R agonism, and that this effect was largely independent of body weight loss [13]. Further, tirzepatide was found to mediate this through engagement of the GIPR, and the effect was accompanied by a reduction in circulating levels of BCAAs and BCKAs [13]. Mechanistically, consistent with the expression profile of the GIPR [13], these whole-body effects are associated with induction of genes linked with the catabolism of BCAAs in brown adipose tissue (BAT), including branched-chain amino acid aminotransferase 2 (BCAT2) and branched-chain alpha-keto acid dehydrogenase (BCKDH), which are mitochondrially located enzymes that catalyze the first and second steps of BCAA catabolism, respectively [14].

The importance of these data is highlighted by the strong association between elevated circulating BCAAs/BCKAs, obesity, systemic IR, and T2D that has consistently been reported in man [14,15]. This leads to a hypothesis that tirzepatide may exert its therapeutic benefits, at least in part, by augmenting the oxidation of BCAAs in BAT. Interestingly, consideration of this concept coincides with the re-discovery of BAT in adult humans, which has rejuvenated interest in the therapeutic potential of this thermogenic organ [16]. The primary physiological role of BAT is to help maintain body temperature in response to cold exposure [17]. To perform this demanding physiological role, BAT has a remarkable capacity to oxidize a diverse set of circulating nutrients, including glucose, lipids, and amino acids [18–20]. Intriguingly, recent studies have shown that activation of BAT-induced thermogenesis promotes the clearance of circulating BCAAs in humans and mice [19,21], and conversely, that genetic knockdown of BCKDH in BAT exacerbates diet-induced obesity [19]. Therefore, the primary objective of the current investigation was to determine whether tirzepatide directly promotes the oxidation of BCAAs in BAT. To address this, we employed stable-isotope tracer studies in combination with metabolomic analyses in obese IR mice following chronic treatment with tirzepatide.

Taking this approach, we found that tirzepatide augments the catabolism of BCAAs/BCKAs specifically in BAT, as demonstrated by increased labeling of BCKA-derived metabolites, and increases in levels of byproducts of BCAA breakdown, including glutamate, alanine, and 3-hydroxyisobutyric acid (3-HIB). In addition, tirzepatide increased the levels of multiple essential and non-essential amino acids and several TCA cycle intermediates in BAT. Together, these findings suggest that tirzepatide induces a thermogenic-like metabolite profile in BAT, an effect that may contribute to reduced circulating BCAAs, improved systemic insulin sensitivity and increased metabolic rate in response to chronic treatment of obese mice with tirzepatide.

2. MATERIALS AND METHODS

2.1. Peptide synthesis

Tirzepatide was synthesized at Eli Lilly and Company.

2.2. Mouse GIPR activity

The activities induced by mouse GIP and tirzepatide at the mouse GIPR were compared using a mouse GIPR GTPγS recruitment membrane binding assay, as previously described for the human receptor [22].

2.3. Animal studies

All animals were individually housed in a temperature-controlled (~24 °C) facility with 12h/12h light/dark cycle. Animal protocols were approved by the Eli Lilly and Co. IACUC. All studies were conducted in obese male mice (C57/BL6J). Animals were maintained on a high-fat diet (consisting of 60% fat, D12492; Research Diets) for 16-weeks, with free access to food and water before randomization by weight. Mice received subcutaneous injections with either vehicle (n = 6, 40 mM Tris-HCl pH8) or tirzepatide (10 nmol/kg, n = 6) once a day for 3 or 14-days. The 10 nmol/kg dose of tirzepatide was chosen based on our prior findings that it elicits clear pharmacological responses in *Glp-1r* null mice [13]. Specifically, tirzepatide treatment reduced fasting glucose, enhanced systemic insulin sensitivity (glucose infusion rate in a hyperinsulimic-euglycemic clamp), and improved adipose tissue-specific insulin sensitivity in obese and insulin resistant GLP-1R KO mice, without impacting body weight [13]. In addition, to control for weight driven changes in metabolism, a separate cohort of animals were pair-fed to the same daily food intake as mice dosed with tirzepatide.

2.4. In vivo stable isotope tracing studies

Two-hours after peptide administration, a baseline blood sample was collected by tail snip and animals received an intraperitoneal injection of [U-^{13}C]KIV (100 mg/kg, Cambridge Isotopes), followed by blood sampling from the tail vein at 5, 10, and 20 min. Immediately after the blood collections, the animals were euthanized and tissues were collected, clamp frozen, and stored at −80 °C.

2.5. Metabolomics analyses

Plasma samples (10 μl) were spiked with 0.2 nmol [2,3,4,4,5,5,5-^{2}H$_8$]valine (D8 valine, Sigma) and 0.2 nmol [3-methyl-^{2}H$_3$-3-^{2}H-1,2,3,4-^{13}C$_4$]2-keto-3-methyl-butyrate (M8 KIV, Sigma) as internal standards. Samples were then mixed with 1 ml acetonitrile to precipitate protein by a brief vortex followed by centrifugation at 18,000×*g* for 30 min. The supernatant was transferred to a new Eppendorf tube and dried completely under N_2 gas. The dried residue was derivatized by adding 40 μl 2% methoxamine in pyridine solution and incubated at 40 °C for 90 min 20 μl N-tert-Butyldimethylsilyl-N-methyltrifluoroacetamide was added for a second derivatization at 80 °C for 30 min. The sample was centrifuged for 15 min at 18,000×*g* before GC-MS analysis.

For tissue samples, ~15 mg tissue was spiked with 0.2 nmol D8 valine and 0.2 nmol M8 KIV as internal standards. 400 μl methanol was added to the sample prior to 2-minute homogenization by Tissulyser. 400 μl distilled water and 400 μl chloroform were added into homogenized sample for another 2-minute homogenization. The sample was centrifuged for 20 min at 18,000×*g* and 700 μl supernatant was dried completely under N_2 gas. The dried tissue sample was derivatized using the same protocol as described above for plasma sample processing.

The GC-MS method was adopted from our previous work [23,24]. GC-MS analysis was performed on an Agilent 7890B GC system equipped with a HP-5MS capillary column (30 m, 0.25 mmi.d., 0.25 mm-phase thickness; Agilent J&W Scientific, Santa Clara, CA), connected to an Agilent 5977A Mass Spectrometer operating under ionization by electron impact (EI) at 70 eV. Helium flow was maintained at 1 mL/min. The temperatures of source, MS quad, interface, and inlet were set at 230, 150, 280, and 250 °C, respectively. Mass spectra were recorded in mass scan mode with *m/z* from 50 to 700. The stable isotope labeling of all measured metabolites was corrected for natural isotope distribution as previously described [25,26].

The absolute concentrations of metabolites reported in Figure 1, Figure 2E–H, Figure 3 A, D, and E, and Figures 4 and 5 were quantified by GC/MS using external calibration curves of standard compounds (0.002–4 nmol), with either M8 KIV or M8 valine as internal standards. M8 KIV was the internal standard for pyruvate and KIV quantification. M8 valine was the internal standard for other metabolites. Absolute concentrations of metabolites reported in Figures 2I, 3B, and 3C were obtained by targeted MS/MS (urea cycle intermediates) or targeted GC/MS methods (TCA cycle intermediates) as previously described, with inclusion of appropriate stable isotope-labeled internal standards (14).

2.6. Amino acid analysis

For data in Figure 6, amino acids were measured using a mass spectrometry–based targeted approach. Brown adipose tissue biopsies were flash frozen in liquid nitrogen immediately after collection and stored at −80 °C until LC-MS/MS analysis. Frozen tissue samples were homogenized with isopropanol using a tissue lyzer. An appropriate volume of isopropanol was added to reach a final concentration of 100 mg/mL. The homogenates were centrifuged for 15 min at 4000 rpm at 4 °C. An aliquot of 25 μL of supernatant was transferred in a PCR 96-well plate and 150 μL of acetonitrile-methanol 1:1 v/v% extraction solution was added. The extraction solution was spiked with a mix of stable labeled internal standards. Samples were mixed thoroughly and incubated at −20 °C overnight. Sample extracts were then centrifuged for 15 min at 4000 rpm at 4 °C and an aliquot of the supernatant was transferred into a new PCR 96-well plate, further diluted 1:1 with the extraction solution, and injected for LC-MS/MS analysis. A pooled calibrator sample was also created by combining an aliquot of the same volume from all the extracted samples together. The pooled calibrator was serially diluted in the extraction solution and used to create a calibration curve (100% (pooled calibrator), 75%, 60%, 40%, 25%, 10%) for relative quantitation. High-, medium-, and low-quality control samples were also prepared at 85%, 50%, and 15%). Amino acid data were acquired using a Shidmadzu Nexera X2 UHPLC system coupled to an AB SCIEX 6500+ triple quadrupole mass spectrometer equipped with an electrospray source. Liquid chromatography was performed using a Waters Acquity BEH Amide (150 mm × 2.1 mm x 3.5 μm particle size) column maintained at 40 °C. Elution solvents were 10 mM ammonium formate adjusted with 0.1% formic acid and 0.1% formic acid in acetonitrile. The mobile phases eluted following a linear gradient. Data were acquired using scheduled

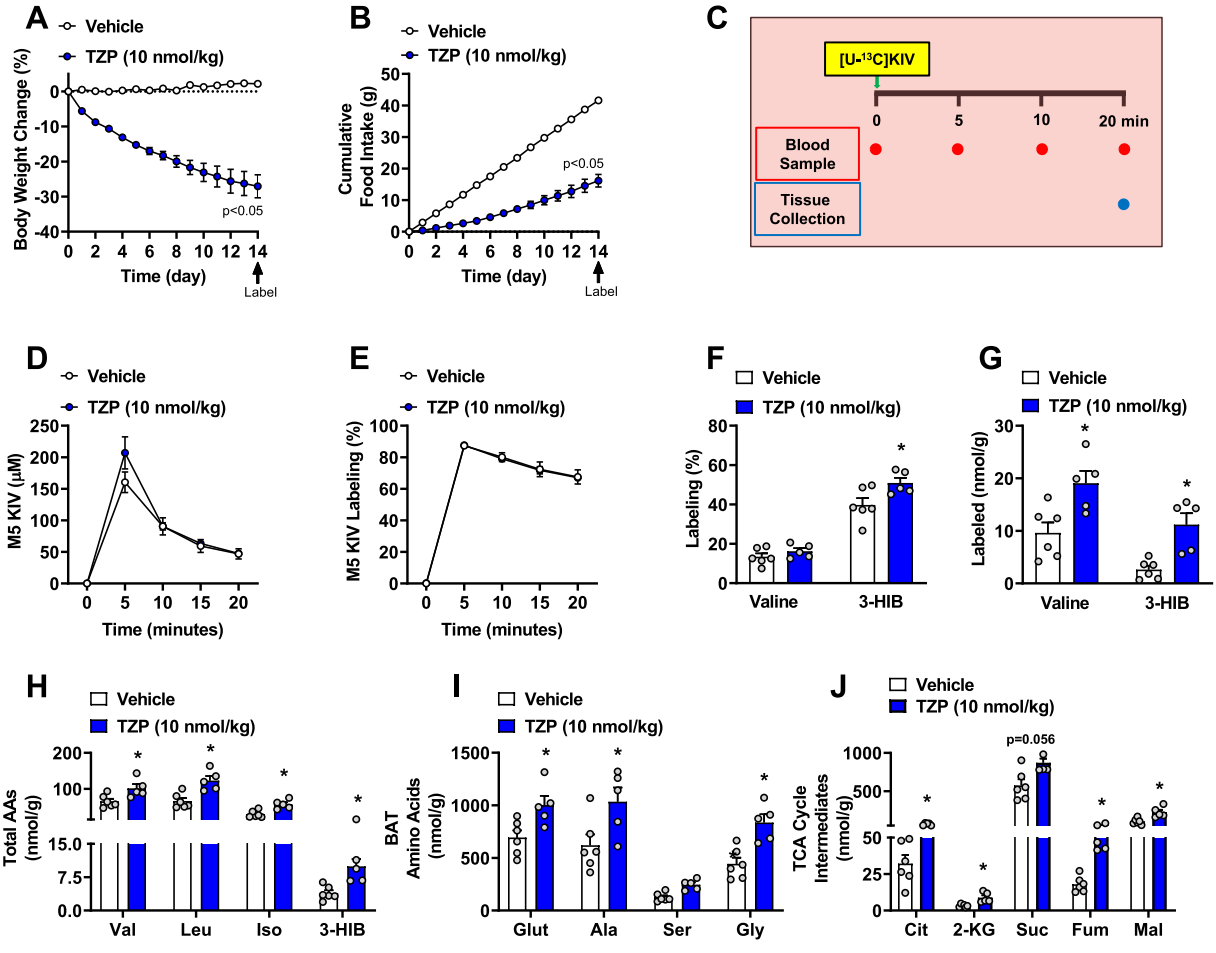

Figure 1: Tirzepatide augments the catabolism of branched-chain amino acids (BCAAs) in brown adipose tissue (BAT). Obese insulin resistant mice were dosed once daily for 14-days with vehicle or tirzepatide (TZP (10 nmol/kg), n = 6 per group). Daily body weight (A) and food intake (B). Schematic representation of uniformally-^{13}C labelled alpha-ketoisovalerat (KIV, [U-13C]KIV) administration protocol (C). Plasma labeling (% and absolute amount) of [U-13C]KIV (D and E). The percentage of labelled valine and 3-HIB in BAT (F). The absolute amounts of labelled valine and 3-hydroxyisobutyrate (3-HIB) in BAT (G). The absolute amounts of unlabeled valine, leucine, isoleucine, 3-HIB (H), glutamate, alanine, serine and glycine (I) citrate (Cit), alpha-keto glutarate (2-KG), succinate, fumarate (Fum) and malate (Mal) in BAT (J). Data are presented as mean ± SEM. Statistical analyses performed included student unpaired t-test (F-J), two-way ANOVA (A, B, D and E), followed by Dunnett's multiple comparisons test where appropriate, *p < 0.05.

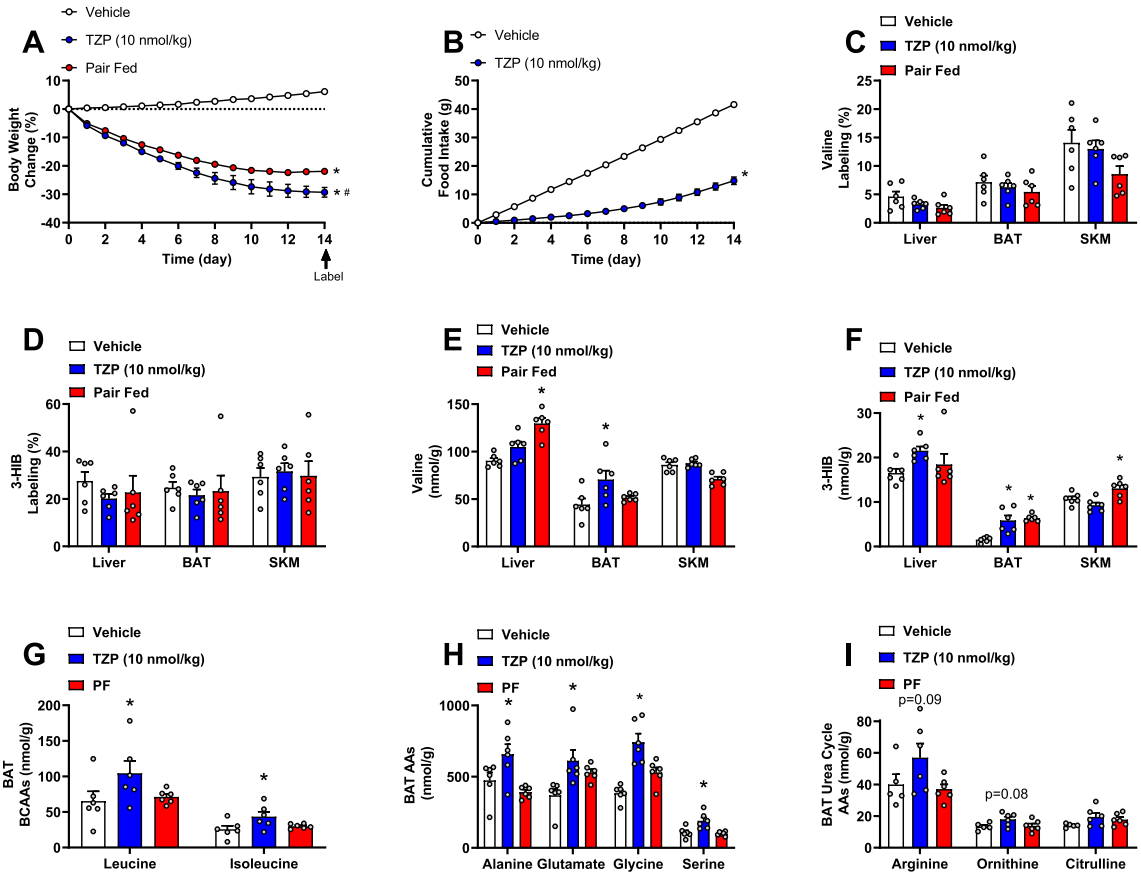

Figure 2: Tirzepatide augments catabolism of branched-chain amino acids (BCAAs) in brown adipose tissue (BAT) independent of weight loss. Obese insulin resistant mice were dosed with vehicle, tirzepatide (TZP (10 nmol/kg)) or pair-fed to TZP daily for 14-days, n = 6 per group. Daily body weight (**A**) and food intake (**B**). The percentage of labelled valine and 3-HIB in liver, BAT and skeletal muscle (SKM, **C and D**). The absolute amounts of unlabeled valine, 3-HIB, leucine, isoleucine, alanine, glutamate, glycine, serine and urea cycle intermediates citrulline, ornithine and arginine in BAT (**E-I**). Data are presented as mean ± SEM. Statistical analyses performed included two-way ANOVA (**A and B**) and one-way ANAOVA (**C-I**) followed by Dunnett's multiple comparisons test where appropriate, *$p < 0.05$ vs vehicle, $^{\#}p < 0.05$ vs pair-fed.

multiple reaction monitoring mode. All ions were monitored as protonated species ($[M+H]^+$). For most amino acids, identification was supported by one qualifier ion monitored in addition to a quantifier ion. Only analytes detected at the lowest pooled calibrator with signal-to-noise > 3 and detected in more than 75% of the individual samples were quantified. Relative quantitation was achieved using a 4 PL regression model using PRISM 8 (San Diego, CA, USA). Peak areas were integrated using the AB SCIEX MultiQuant 3.0.2 software. A total of 36 samples was submitted to statistical analysis, 6 samples per treatment group (vehicle, tirzepatide 10 nmol/kg (TZP 10 nmol/kg), pair-fed to tirzepatide (PF)) for two timepoints (day 3 and day 14). For statistical analysis, amino acid data were log-transformed. One-way analysis of variance (ANOVA) was performed to assess significance (unadjusted $P < 0.05$) between group data distributions. Fold changes and standard errors were computed between treatment groups (TZP 10 nmol/kg and PF) and vehicle. Heatmaps were generated using log2 transformation of least square means (LSm) using R 3.6.0. Figures were edited using Adobe Photoshop 2020.

2.7. Statistical analysis

Data are presented as mean ± SEM. Statistical analyses performed included student unpaired t-test, one-way ANOVA or two-way ANOVA, followed by Dunnett's multiple comparisons test where appropriate. Differences were considered significant when $p < 0.05$*.

3. RESULTS

3.1. Tirzepatide promotes BCAA catabolism in BAT

In previous studies, we observed that treatment with tirzepatide reduces circulating concentrations of BCAAs and BCKAs in obese mice and in humans [12], while augmenting BCAA catabolic gene expression in BAT collected from obese IR mice [13]. Therefore, to determine whether tirzepatide promotes the uptake and catabolism of BCAAs in BAT, *in vivo* stable-isotope tracing was used to investigate BCAA metabolism in obese mice that had been dosed daily for two weeks with vehicle or tirzepatide. A dose of 10 nmol/kg of tirzepatide was used in this study because we previously found it to elicit a suite of pharmacological responses in *Glp1r* null mice [13]. Specifically, 10 nmol/kg of tirzepatide reduced fasting glucose, enhanced systemic insulin sensitivity (glucose infusion rate in a hyperinsulinemic-euglycemic clamp), and improved adipose tissue-specific insulin sensitivity in obese and insulin resistant *Glp-1rKO* mice, without impacting body weight [13].

Human GIP is known to have weaker affinity for the mouse GIPR compared to the human GIPR [27]. To further and more formally investigate the ability of tirzepatide to activate the mouse GIPR, we compared the effects of tirzepatide and mouse GIP (mGIP) using a mGIPR GTPγS recruitment membrane binding assay [22]. As anticipated, mGIP was approximately 20-fold more potent than tirzepatide

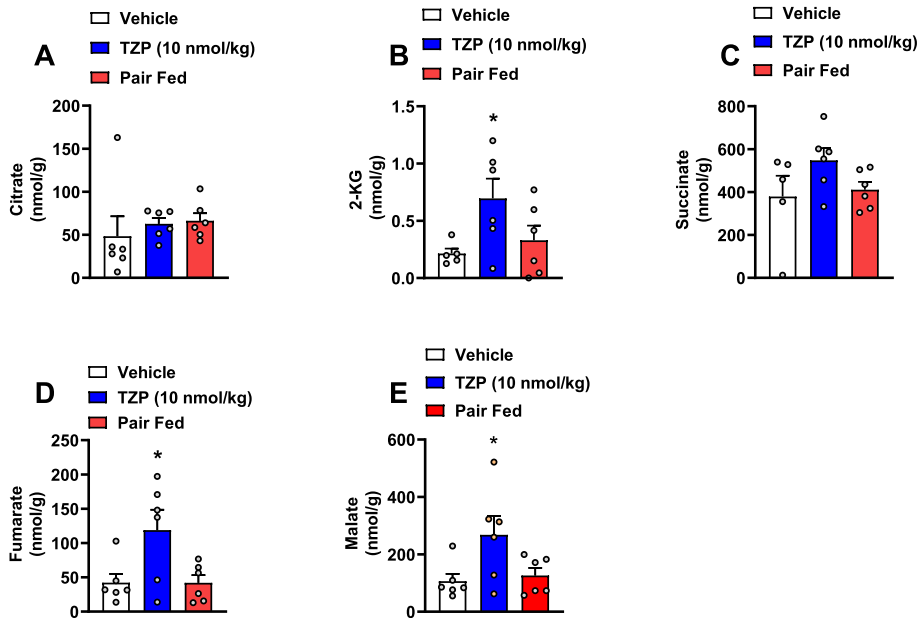

Figure 3: Tirzepatide increases TCA cycle intermediate levels in brown adipose tissue independent of weight loss. Obese insulin resistant mice were dosed with vehicle, tirzepatide (TZP (10 nmol/kg)) or pair-fed to TZP daily for 14-days, n = 6 per group. The absolute amounts of citrate (**A**), alpha-ketoglutarate (2-KG, **B**), succinate (**C**), fumarate (**D**) and malate (**E**) content in BAT (**G** and **H**). Data are presented as mean ± SEM. Statistical analysis was performed using a one-way ANAOVA followed by Dunnett's multiple comparisons test where appropriate, *p < 0.05.

(Supplemental Figure 1A) in this assay. This finding aligns with the original engineering of tirzepatide to target the human GIPR [28], but also confirms a capacity for tirzepatide to activate the mouse GIPR, albeit with lesser potency.

As expected, a significant decrease in body weight and food intake was observed in animals treated with tirzepatide (Figure 1A,B). Following the treatment period, animals received an intravenous injection of uniformally-^{13}C-labeled ketoisovalerate ([U-^{13}C]KIV), the α-ketoacid of valine, followed by blood sampling from the tail vein at 5, 15, and 20 min for measurement of metabolite levels and labeling, using mass spectrometry (Figure 1C). The α-ketoacid of valine was utilized in our study because it serves as the immediate substrate for the rate-determining step in BCAA catabolism, BCKDH. Use of the labeled ketoacid also allowed us to track labeling of ^{13}C-labeled valine and ^{13}C-labeled 3-HIB in BAT, serving as markers of KIV reamination and catabolism, respectively. Consistent with previous findings [29,30], there was a rapid rise and decline in the total plasma [U-^{13}C]KIV pool in both vehicle and tirzepatide treated mice (Figure 1D). Strikingly, within 5-min of label administration, 80% of the plasma KIV pool was labelled (Figure 1E). Further, by 20-min, plasma [U-^{13}C]KIV had returned to near-baseline levels (Figure 1D). There was no effect of tirzepatide relative to vehicle on the clearance of plasma [U-^{13}C]KIV in this time frame (Figure 1D,E). To evaluate the impact of tirzepatide on BCAA catabolism, we examined ^{13}C enrichment of BCAA/BCKA-derived metabolites in BAT. In vehicle-treated mice, there was robust ^{13}C labelling of the valine and 3-HIB pools in BAT 20-min after [U-^{13}C]KIV administration (Figure 1F). Tirzepatide significantly increased percent labelling of 3-HIB (Figure 1F), and increased the total labeled pool of valine (19.05 ± 2.14 nmol/g and 9.61 ± 1.98 nmol/g for tirzepatide and vehicle, respectively) and 3-HIB (11.19 ± 1.96 nmol/g and 2.62 ±

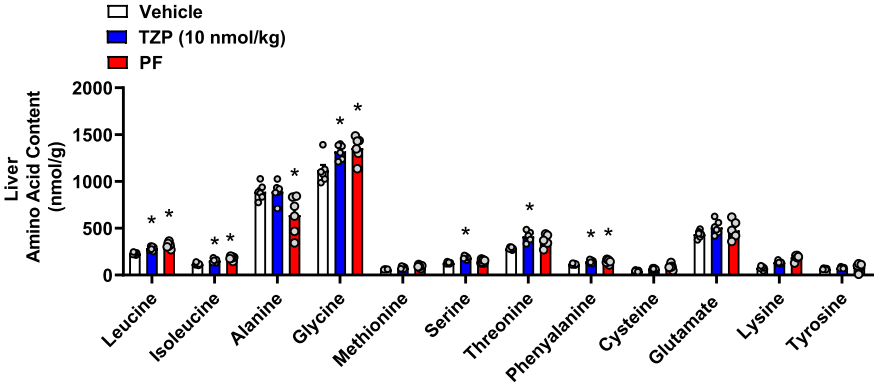

Figure 4: Chronic treatment with tirzepatide increases amino acid content in the liver in a weight-dependent manner. Obese insulin resistant mice were dosed with vehicle, tirzepatide (TZP (10 nmol/kg)) or pair-fed to TZP daily for 14-days, n = 6 per group. The absolute amino acid content in the liver. Data are presented as mean ± SEM. Statistical analysis was performed using a one-way ANAOVA followed by Dunnett's multiple comparisons test where appropriate, *p < 0.05.

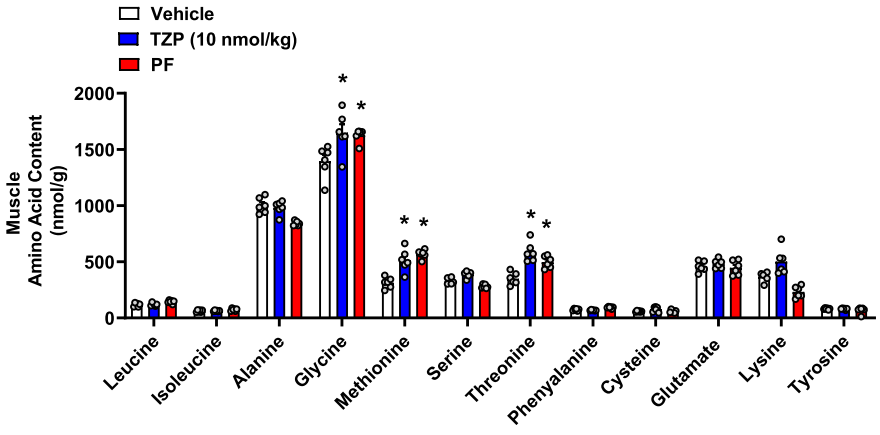

Figure 5: Chronic treatment with tirzepatide augments amino acid content in skeletal muscle in a weight-dependent manner. Obese insulin resistant mice were dosed with vehicle, tirzepatide (TZP (10 nmol/kg)) or pair-fed to TZP daily for 14-days, n = 6 per group. The absolute amino acid content in skeletal muscle. Data are presented as mean ± SEM. Statistical analysis was performed using a one-way ANAOVA followed by Dunnett's multiple comparisons test where appropriate, *p < 0.05.

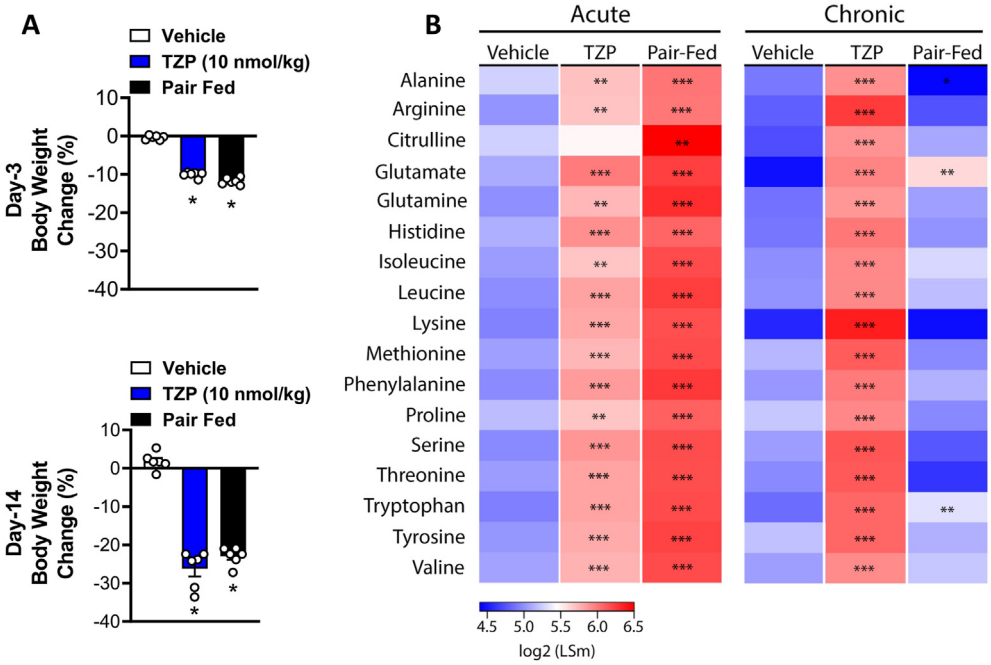

Figure 6: Chronic Treatment with Tirzepatide induces a thermogenic-like amino acid profile in brown adipose tissue (BAT). Obese insulin resistant mice were dosed with vehicle, tirzepatide (TZP (10 nmol/kg)) or pair-fed to TZP daily for 3 or 14-days, n = 6 per group. Effect of TZP on body weight (**A**) and tissue levels of BCAAs in BAT (**B**). Statistical analyses performed included one-way ANOVA and two-way ANOVA. *Unadjusted P < 0.05. **Unadjusted P < 0.01, ***Unadjusted P < 0.001.

0.73 nmol/g for tirzepatide and vehicle, respectively) in BAT (Figure 1G), indicating enhanced KIV reamination and catabolism, respectively. Further, chronic administration of tirzepatide increased total levels of valine, leucine, isoleucine and 3-HIB (Figure 1H), as well as levels of other amino acids linked with BCAA catabolism such as glutamate, alanine, glycine, and serine (Figure 1I) in BAT. The catabolism of BCAAs has been shown to directly (via generation of acetyl-CoA) or indirectly (through anapleorosis) contribute to the generation of TCA cycle intermediates and thereby metabolic flux in BAT [19,30], and we found that tirzepatide treatment raised malate, citrate, fumarate, succinate, and a-ketoglutarate levels in BAT (Figure 1J). Collectively, these experiments support the notion that tirzepatide promotes systemic clearance of BCAA in obese mice via catabolism of these substrates in BAT.

3.2. Tirzepatide augments BCAA catabolism in BAT independent of weight loss

Since the impact of tirzepatide on BCAA catabolism in BAT could be driven by its effect on caloric intake and/or body weight, we added a pair-feeding arm to an independent tirzepatide treatment arm and repeated a subset of the metabolic measurements. Obese mice were pair-fed (PF) to the same daily food intake as animals dosed with tirzepatide. Chronic treatment with tirzepatide and PF reduced body weight to a similar extent (Figure 2A,B). Following the two-week

intervention period, mice received an intravenous injection of [U-^{13}C] KIV, and 20-min after label administration, organs were harvested for measurement of ^{13}C enrichment of various metabolites. There was robust ^{13}C labelling of the valine and 3-HIB pools in liver, skeletal muscle, and BAT across all experimental groups (Figure 2C,D). Consistent with results summarized in Figure 1, tirzepatide treatment resulted in significant increases of the total levels of valine, 3-HIB (Figure 2E,F), leucine, and isoleucine in BAT (Figure 2G) relative to the vehicle control group. Tirzepatide treatment also raised the content of the BCAA catabolic products glutamate, serine, and alanine (Figure 2H), as well as the urea cycle intermediates citrulline and ornithine (Figure 2I) in BAT. Among all of these analytes, the only one increased significantly by PF in BAT was 3-HIB (Figure 2F). Further, we found that chronic treatment with tirzepatide, but not PF, robustly augmented levels of the TCA cycle intermediates α-ketoglutarate, fumarate, and malate in BAT (Figure 3A—E). Overall, these results suggest that the effect of tirzepatide treatment on BCAA metabolism in BAT is largely independent of its effects on food intake and body weight.

Caloric restriction may augment the catabolism of BCAAs in the liver and skeletal muscle. It was therefore important to determine whether the food intake/weight-independent effects of tirzepatide treatment on BCAA metabolism are specific to BAT. To investigate this, we evaluated the metabolic impact of tirzepatide and pair-feeding in the liver and skeletal muscle (Figures 4 and 5). Notably, tirzepatide and pair-feeding had similar effects on BCAA levels and other amino acid species in these tissues (Figures 4 and 5). Specifically, in the liver, both tirzepatide treatment and pair-feeding resulted in increased levels of leucine, isoleucine, glycine, serine, and phenylalanine (Figure 4), while in skeletal muscle, glycine, methione, and threonine levels were elevated by both interventions (Figure 5). There was no effect of tirzepatide on levels of any of these amino acids in subcutaneous WAT (Supplemental Figure 1B). Together, these results suggest that weight-independent effects of tirzepatide treatment on BCAA catabolism occur mainly in BAT. The data also suggest that the effects of tirzepatide on liver and skeletal muscle amino acid metabolism may be secondary to the common effects of the drug and pair-feeding to lower body weight and affect energy balance.

The thermogenic activity of BAT is characterized by the uptake and oxidation of glucose, lipids, and amino acids [31]. Thus, we next sought to determine whether the impact of tirzepatide treatment on amino acid metabolism is specific to the BCAA catabolic pathway (valine, leucine, isoleucine, 3-HIB, glutamate, alanine, glycine, and serine), or whether it involves other amino acid species known to be oxidized in BAT in response to enhanced energetic demand [32]. To address this, metabolomics analysis was applied to BAT collected from tirzepatide-treated obese mice in a time-course study design that included a pair-feeding arm to help disentangle both the time and weight/food intake-dependent effects of tirzepatide on amino acid content in BAT. Over the first 72 h of intervention, weight loss was identical in animals treated with tirzepatide compared with the pair-fed group (Figure 6A). Over this time frame, both tirzepatide and PF resulted in increased tissue content of BCAAs (valine, leucine, and isoleucine) and their catabolic byproducts (glutamate, alanine, and serine) (Figure 6B). Strikingly, both interventions also resulted in an increase in levels of a set of essential (histamine, lysine, phenylalanine, methione, threonine, and tryptophan) and non-essential (proline, serine, tyrosine, alanine, arginine, citrulline, and glutamine) amino acids.

In contrast to the effects of acute treatment, chronic treatment with tirzepatide over 14 days had a distinct impact on amino acid levels in BAT when compared to the PF group despite a similar reduction in body weight between the two groups (Figure 6A). As expected tirzepatide, but not PF, robustly increased BCAA levels in BAT relative to control or PF animals (Figure 6B). Further, tirzepatide treatment augmented the levels of several other amino acid species, including arginine, citrulline, histidine, lysine, methionine, phenylalanine, proline, threonine, tryptophan, and tyrosine relative to either the PF or vehicle-treated group (Figure 6B). Collectively, these studies indicate that following chronic treatment, tirzepatide increases the levels of several amino acid species in BAT, an effect that appears to be largely independent of food intake and body weight. We note that the amino acid signature found in BAT following chronic treatment with tirzepatide is reminiscent of the amino acid profile that occurs in BAT following cold exposure, a condition where amino acid uptake is increased to achieve optimal thermogenic capacity [19,32].

4. DISCUSSION

Treatment with the dual GIP and GLP-1 receptor agonist tirzepatide provides weight-dependent and -independent insulin sensitization in patients with T2D [10]. In previous studies in humans and mice, we found that tirzepatide-mediated weight-independent insulin sensitization is associated with a reduction in circulating BCAAs/BCKAs, effects coupled in mice with induction of a BCAA catabolic program in BAT [13]. Here, we have made direct measurements of BCKA metabolism by applying *in vivo* stable-isotope tracer studies in combination with metabolomic analyses in obese IR mice. The major findings of this new investigation are that tirzepatide treatment in rodents stimulates the catabolism of BCAAs/BCKAs in BAT. Further, tirzepatide increased the levels of multiple TCA cycle intermediates in BAT, an effect that may be associated with increased anaplerosis. Finally, we report that chronic treatment with tirzepatide raised the levels of multiple amino acids in addition to the BCAAs in BAT, as has also been reported in response to cold exposure [19,33,34]. These findings suggest that tirzepatide is a pharmacologic agent that mimics the effect of cold exposure on the amino acid profile of BAT.

A limitation of our study is that we did not conduct metabolic labeling studies in separate cohorts of mice treated with selective GIPR or GLP-1R agonists. However, our prior work has demonstrated that treatment with a long-acting GIPR agonist caused significant lowering of circulating levels of BCAAs, increased BCAA content in BAT, and induced expression of BCAA catabolic genes in BAT of obese, insulin resistant mice [13]. This prior work establishes, via metabolomic and transcriptomic analyses, that GIPR agonism alone affects BCAA metabolism in BAT in a manner similar to that observed with tirzepatide treatment. In other studies, we have shown that tirzepatide reduces fasting glucose, enhances systemic insulin sensitivity (glucose infusion rate in a hyperinsulimic-euglycemic clamp), and improves adipose tissue-specific insulin sensitivity in obese and insulin resistant GLP-1R KO mice, without impacting body weight [1]. However, given the lower affinity of tirzepatide for the mouse compared to the human GIPR, we cannot presently determine if the selective effect of tirzepatide on glucose homeostasis but not weight loss in GLP-1R KO mice is due to the absence of GLP-1R signaling alone, or the differential potency of tirzepatide on the mouse relative to human GIPR. Follow-up metabolic flux studies with GIPR and/or GLP-1R null mice are needed to definitively elucidate the contribution of each receptor to the effect of tirzepatide on BCAA metabolism.

Dysregulation of BCAA metabolism is associated with obesity and IR and may play a causal role in pathogenesis of T2D [14,35]. Consistent with this, obesity-associated impairments in catabolism of BCAAs/BCKAs in the liver, WAT, and BAT are linked with increased systemic

levels of BCAA/BCKA, while feeding of a BCAA-restricted diet or the induction of BCAA catabolism by pharmacologic or genetic manipulations lowers circulating BCAAs and protects from obesity-induced IR [36–39]. In line with these findings, it has been shown previously that tirzepatide reduces circulating BCAAs in rodents and humans [12], and that treatment with tirzepatide or a long-acting GIPR agonist improved insulin sensitivity, reduced circulating BCAAs/BCKAs, and induced BCAA catabolic gene expression in BAT of obese and insulin resistant mice [13]. These findings led us to hypothesize that treatment with tirzepatide reduces circulating BCAAs by promoting their oxidation in BAT. Indeed, a key finding of the current investigation is that chronic treatment with tirzepatide augments catabolism of the labelled alpha-keto acid of valine, KIV, in BAT from obese IR mice. Specifically, tirzepatide treatment increased ^{13}C labeling of 3-HIB, a product of valine and KIV catabolism in BAT. We also found that treated animals had increased tissue levels of glutamate and alanine, which are generated by transamination of BCAA catalyzed by BCAT2, as well as serine and glycine, which serve as substrates for replenishing pyruvate under conditions of active pyruvate/alanine shuttle activity [40]. Following chronic treatment, the effects on amino acids in BAT occurred largely independent of effects of tirzepatide on body weight, as pair-feeding failed to induce these changes. Interestingly, not only did tirzepatide increase BCAA catabolism in BAT, but it also induced KIV reamination, as measured by increases in labelled valine concentrations in BAT. We have previously demonstrated active reamination of KIV to valine in heart [29], but in light of induction of the enzyme that catalyzes this reaction, BCAT2, in response to tirzepatide treatment in BAT [12], some of this activity measured here may have been contributed by BCAT activity in BAT.

Cold-mediated activation of BAT thermogenesis is known to stimulate clearance of BCAAs in mice and humans [19,32–34], while BAT-specific deletion of BCKDH in mice impairs cold-induced thermogenesis, driving weight gain and impaired glycemic control [19]. Further, BAT is reported to account for a major proportion (19%) of whole-body BCAA (isoleucine) oxidation [30], and the contribution of BCAA to succinate synthesis drives both activation and maintenance of BAT-induced thermogenesis in mice [21]. Together, these findings support the hypothesis that chronic treatment with tirzepatide promotes the oxidation of circulating BCAAs/BCKAs primarily in BAT, an effect that mimics cold exposure.

BAT-induced thermogenesis requires a constant supply of energy-producing substrates [31]. To meet this energetic need, BAT is known to import and oxidize several amino acid species, in addition to BCAAs, in response to cold exposure [32–34]. The TCA cycle is a central pathway linking the catabolism of energy substrates to the electron transport system [41,42]. Previously, we showed that treatment with tirzepatide induces the expression of thermogenic genes in BAT (e.g., UCP-1), and that this effect is coupled with the recruitment of genes encoding proteins that facilitate mitochondrial transport of amino acids (e.g., SLC25139, SLC25A29, and SLC25A22) [13]. Our current data shows that tirzepatide induces a cold-like thermogenic amino acid signature in BAT, causing an increase in the levels of several essential (e.g., lysine, phenylalanine, and tryptophan) and non-essential (e.g., alanine, glutamate, glutamine, and proline) amino acids known to be elevated in thermogenically active BAT [32–34]. The augmentation of amino acid content by tirzepatide in BAT may: 1) facilitate the delivery of energetic substrates; and 2) provide anaplerotic intermediates that feed the TCA cycle (phenylalanine and tyrosine to produce fumarate; methione to produce succinyl-CoA; and glutamine, proline, and histidine to produce α-KG [42]). Indeed, a key observation of the current investigation is that chronic treatment with tirzepatide increases the levels of multiple TCA cycle intermediates, including succinate, fumarate, malate, and α-KG in BAT. These effects are not observed in animals pair-fed to food intake of the tirzepatide-treated mice, but we note that weight loss was not exactly matched in the pair-fed versus tirzepatide-treated groups used to generate the data in Figure 6. Thus, our results are consistent with the major effects of tirzepatide on metabolic profile of BAT occurring via a weight loss-independent mechanism, but with a possibility of a small contribution of a weight-dependent effect. Also, it remains possible given the relatively lower activity of tirzepatide versus mGIP on the mouse GIPR that a higher dose (>10 nmol/kg) of tirzepatide could even further impact body weight, a phenomenon that may be best investigated in obese wild-type compared to *Glp-1r* KO mice. Stated another way, at the 10 nmol/kg dose of tirzepatide used in the current study, it is unclear if weight lowering effects that might be mediated by the mGIPR were fully engaged, resulting in a possible underestimate of the overall therapeutic impact of tirzepatide in the context of the mouse model studied here.

The utilization of amino acids as energetic substrates requires efficient disposal of ammonia (NH_3). To ensure safe delivery of excess nitrogen to the urea cycle in the liver, several amino acid species (for example, alanine, glutamine, glutamine, and proline) function as nitrogen donors [43]. Here, we found that tirzepatide increases the levels of alanine, glutamate, proline, and glutamine in BAT. Whereas urea cycle enzymes are known to be enriched in the liver, extra-hepatic nitrogen disposal mechanisms may be induced under conditions of enhanced amino acid catabolism [43]. Interestingly, we found that in addition to causing increases in amino acids that shuttle nitrogen out of tissues (alanine, glutamine, and proline), chronic treatment with tirzepatide also led to near-significant increases in levels of urea cycle intermediates (citrulline and ornithine) in BAT. This suggests the possibility that tirzepatide induces extra-hepatic nitrogen utilization mechanisms in BAT to help ensure rapid disposal of nitrogen during augmented BAT-induced thermogenesis. Further investigation will be needed to address this possibility.

In summary, we report that treatment with the dual GIP and GLP-1 receptor agonist tirzepatide impacts the amino acid profile of key metabolic organs. Specifically, tirzepatide selectively promotes BCKA metabolism in BAT compared to other tissues, an effect that appears to be driven in both a weight-dependent and independent manner. Further, chronic tirzepatide treatment raises the levels of multiple amino acid species in addition to BCAAs that are also elevated in BAT in response to cold exposure. Finally, chronic treatment with tirzepatide increases tissue levels of several TCA intermediates, suggesting enhanced production of both oxidative and anaplerotic TCA cycle substrates. Together, these findings suggest that tirzepatide induces a thermogenic-like amino acid profile in BAT, an effect that may contribute to the benefits of tirzepatide treatment in obese mice, including improved insulin sensitization, increased metabolic rate, and weight loss. Of note, considering the differential activity of mouse GIP and tirzepatide at the mouse GIPR, our studies in mice may have underestimated the metabolic benefits of tirzepatide. Future mechanistic studies in human subjects are needed to fully investigate this issue.

AUTHOR CONTRIBUTIONS

B.A.D, **E.C.F** and **S.B** performed all *in vivo* studies and stable isotope tracing studies.
G.F.Z, **K.A.C**, **V.P**, **W.H**, **and O.I** performed metabolomic analysis and contributed to data interpretation.
G.F.Z, **K.W.S**, **T.C and J.T.B** contributed to the study design, and data interpretation.
C.S conducted mouse GIPR activity assays
R.J.S. **and C.B.N** were responsible for study conception, experimental designs, data analyses and interpretation.
R.J.S, **G.F.Z**, **K.W.S and C.B.N** wrote the manuscript

DATA AVAILABILITY

Data will be made available on request.

CONFLICT OF INTEREST

R.J.S, V.P, K.A.C, Y.L, E.C.F, B.A.D, S.M., T.C, K.W.S, J.B, are current or past employees of Eli Lilly and Company. All work reported here was supported by Eli Lilly and Company, including studies conducted at Duke under a sponsored research agreement to C.B.N and G.F.Z. C.B.N. is a member of the Lilly Global Diabetes Advisory Board.

APPENDIX A. SUPPLEMENTARY DATA

Supplementary data to this article can be found online at https://doi.org/10.1016/j.molmet.2022.101550.

REFERENCES

[1] Blüher, M., 2019. Obesity: global epidemiology and pathogenesis. Nature Reviews Endocrinology 15(5):288–298.
[2] Zimmet, P., Alberti, K.G., Magliano, D.J., Bennett, P.H., 2016. Diabetes mellitus statistics on prevalence and mortality: facts and fallacies. Nature Reviews Endocrinology 12(10):616–622.
[3] Sloop, K.W., Emmerson, P.J., Statnick, M.A., Willard, F.S., 2018. The current state of GPCR-based drug discovery to treat metabolic disease. British Journal of Pharmacology 175(21):4060–4071.
[4] Tschöp, M.H., Finan, B., Clemmensen, C., Gelfanov, V., Perez-Tilve, D., Müller, T.D., et al., 2016. Unimolecular polypharmacy for treatment of diabetes and obesity. Cell Metabolism 24(1):51–62.
[5] Samms, R.J., Coghlan, M.P., Sloop, K.W., 2020. How may GIP enhance the therapeutic efficacy of GLP-1? Trends in Endocrinology and Metabolism 31(6):410–421.
[6] Frias, J.P., 2020. Tirzepatide: a glucose-dependent insulinotropic polypeptide (GIP) and glucagon-like peptide-1 (GLP-1) dual agonist in development for the treatment of type 2 diabetes. Expert Review of Endocrinology and Metabolism 15(6):379–394.
[7] Frías, J.P., Davies, M.J., Rosenstock, J., Pérez Manghi, F.C., Fernández Landó, L., Bergman, B.K., et al., 2021. Tirzepatide versus semaglutide once weekly in patients with type 2 diabetes. New England Journal of Medicine 385(6):503–515.
[8] Delahanty, L.M., Pan, Q., Jablonski, K.A., Aroda, V.R., Watson, K.E., Bray, G.A., et al., 2014. Effects of weight loss, weight cycling, and weight loss maintenance on diabetes incidence and change in cardiometabolic traits in the Diabetes Prevention Program. Diabetes Care 37(10):2738–2745.
[9] Wilding, J.P.H., 2014. The importance of weight management in type 2 diabetes mellitus. International Journal of Clinical Practice 68(6):682–691.
[10] Thomas, M.K., Nikooienejad, A., Bray, R., Cui, X., Wilson, J., Duffin, K., et al., 2021. Dual GIP and GLP-1 receptor agonist tirzepatide improves beta-cell function and insulin sensitivity in type 2 diabetes. Journal of Clinical Endocrinology & Metabolism 106(2):388–396.
[11] Wilson, J.M., Nikooienejad, A., Robins, D.A., Roell, W.C., Riesmeyer, J.S., Haupt, A., et al., 2020. The dual glucose-dependent insulinotropic peptide and glucagon-like peptide-1 receptor agonist, tirzepatide, improves lipoprotein biomarkers associated with insulin resistance and cardiovascular risk in patients with type 2 diabetes. Diabetes, Obesity and Metabolism 22(12):2451–2459.
[12] Pirro, V., et al., 2022. Effects of tirzepatide, a dual GIP and GLP-1 RA, on lipid and metabolite profiles in subjects with type 2 diabetes. Journal of Clinical Endocrinology & Metabolism 107(2):363–378.
[13] Samms, R.J., Christe, M.E., Colllins, K.A., Pirro, V., Droz, B.A., Holland, A.K., et al., 2021. GIPR agonism mediates weight-independent insulin sensitization by tirzepatide in obese mice. Journal of Clinical Investigation 131(12):e146353.
[14] White, P.J., McGarrah, R.W., Herman, M.A., Bain, J.R., Shah, S.H., Newgard, C.B., 2021. Insulin action, type 2 diabetes, and branched-chain amino acids: a two-way street. Molecular Metabolism 101261.
[15] Newgard, C.B., Jie An, J., Bain, J.R., Muehlbauer, M.J., Stevens, R.D., Lien, L.F., et al., 2009. A branched-chain amino acid-related metabolic signature that differentiates obese and lean humans and contributes to insulin resistance. Cell Metabolism 9(4):311–326.
[16] Nedergaard, J., Cannon, B., 2010. The changed metabolic world with human brown adipose tissue: therapeutic visions. Cell Metabolism 11(4):268–272.
[17] Cannon, B., Nedergaard, J., 2004. Brown adipose tissue: function and physiological significance. Physiological Reviews 84(1):277–359.
[18] Bartelt, A., Bruns, O.T., Reimer, R., Hohenberg, H., Ittrich, H., Peldschus, K., et al., 2011. Brown adipose tissue activity controls triglyceride clearance. Nature Medicine 17(2):200–205.
[19] Yoneshiro, T., Wang, Q., Tajima, K., Matsushita, M., Maki, H., Igarashi, K., et al., 2019. BCAA catabolism in brown fat controls energy homeostasis through SLC25A44. Nature 572(7771):614–619.
[20] Stanford, K.I., Middelbeek, R.J.W., Townsend, K.L., An, D., Nygaard, E.B., Hitchcox, K.M., et al., 2013. Brown adipose tissue regulates glucose homeostasis and insulin sensitivity. Journal of Clinical Investigation 123(1):215–223.
[21] Yoneshiro, T., Kataoka, N., Walejko, J.M., Ikeda, K., Brown, Z., Yoneshiro, M., et al., 2021. Metabolic flexibility via mitochondrial BCAA carrier SLC25A44 is required for optimal fever. Elife 10:e66865.
[22] Willard, F.S., Douros, J.D., Gabe, M.B., Showalter, A.D., Wainscott, D.B., Suter, T.M., et al., 2020. Tirzepatide is an imbalanced and biased dual GIP and GLP-1 receptor agonist. JCI Insight 5(17):e140532.
[23] Wang, Y., Christopher, B.A., Wilson, K.A., Muoio, D., McGarrah, R.W., Brunengraber, H., et al., 2018. Propionate-induced changes in cardiac metabolism, notably CoA trapping, are not altered by l-carnitine. American Journal of Physiology. Endocrinology and Metabolism 315(4):E622–E633.
[24] Zhang, G.F., Jensen, M.V., Gray, S.M., El, K., Wang, Y., Lu, D., et al., 2021. Reductive TCA cycle metabolism fuels glutamine- and glucose-stimulated insulin secretion. Cell Metabolism 33(4):804–817 e5.
[25] Fernandez, C.A., Des Rosiers, C., Previs, S.F., David, F., Brunengraber, H., 1996. Correction of 13C mass isotopomer distributions for natural stable isotope abundance. Journal of Mass Spectrometry 31(3):255–262.
[26] Tomcik, K., Ibarra, R.A., Sadhukhan, S., Han, Y., Tochtrop, G.P., Zhang, G.-F., 2011. Isotopomer enrichment assay for very short chain fatty acids and its metabolic applications. Analytical Biochemistry 410(1):110–117.
[27] Mroz, P.A., Finan, B., Gelfanov, V., Yang, B., Tschöp, M.H., DiMarchi, R.D., et al., 2019. Optimized GIP analogs promote body weight lowering in mice through GIPR agonism not antagonism. Molecular Metabolism 20:51–62.

[28] Coskun, T., Sloop, K.W., Loghin, C., Alsina-Fernandez, J., Urva, S., Bokvist, K.B., et al., 2018. LY3298176, a novel dual GIP and GLP-1 receptor agonist for the treatment of type 2 diabetes mellitus: from discovery to clinical proof of concept. Molecular Metabolism 18:3—14.

[29] Walejko, J.M., Christopher, B.A., Crown, S.B., Zhang, G.-F., Pickar-Oliver, A., Yoneshiro, T., et al., 2021. Branched-chain α-ketoacids are preferentially reaminated and activate protein synthesis in the heart. Nature Communications 12(1):1680.

[30] Neinast, M.D., Jang, C., Hui, S., Murashige, D.S., Chu, Q., Morscher, R.J., et al., 2019. Quantitative analysis of the whole-body metabolic fate of branched-chain amino acids. Cell Metabolism 29(2):417—429 e4.

[31] Townsend, K.L., Tseng, Y.H., 2014. Brown fat fuel utilization and thermogenesis. Trends in Endocrinology and Metabolism 25(4):168—177.

[32] López-Soriano, F.J., Fernández-López, J.A., Mampel, T., Villarroya, F., Iglesias, R., Alemany, M., et al., 1988. Amino acid and glucose uptake by rat brown adipose tissue. Effect of cold-exposure and acclimation. Biochemical Journal 252(3):843—849.

[33] Okamatsu-Ogura, Y., Kuroda, M., Tsutsumi, R., Tsubota, A., Saito, M., Kimura, K., et al., 2020. UCP1-dependent and UCP1-independent metabolic changes induced by acute cold exposure in brown adipose tissue of mice. Metabolism 113:154396.

[34] Panic, V., Pearson, S., Banks, J., Tippetts, T.S., Velasco-Silva, J.N., Lee, S., et al., 2020. Mitochondrial pyruvate carrier is required for optimal brown fat thermogenesis. Elife 9:e52558.

[35] White, P.J., Newgard, C.B., 2019. Branched-chain amino acids in disease. Science 363(6427):582—583.

[36] Herman, M.A., She, P., Peroni, O.D., Lynch, C.J., Kahn, B.B., 2010. Adipose tissue branched chain amino acid (BCAA) metabolism modulates circulating BCAA levels. Journal of Biological Chemistry 285(15):11348—11356.

[37] Zhou, M., Shao, J., Wu, C.-Y., Shu, L., Dong, W., Liu, Y., et al., 2019. Targeting BCAA catabolism to treat obesity-associated insulin resistance. Diabetes 68(9):1730—1746.

[38] White, P.J., McGarrah, R.W., Grimsrud, P.A., Tso, S.-C., Yang, W.-H., Haldeman, J.M., et al., 2018. The BCKDH kinase and phosphatase integrate BCAA and lipid metabolism via regulation of ATP-citrate lyase. Cell Metabolism 27(6):1281—1293 e7.

[39] White, P.J., Lapworth, A.L., An, J., Wang, L., McGarrah, R.W., Stevens, R.D., et al., 2016. Branched-chain amino acid restriction in Zucker-fatty rats improves muscle insulin sensitivity by enhancing efficiency of fatty acid oxidation and acyl-glycine export. Molecular Metabolism 5(7):538—551.

[40] White, P.J., Lapworth, A.L., McGarrah, R.W., Coulter Kwee, L., Crown, S.B., Ilkayeva, O., et al., 2020. Muscle-liver trafficking of BCAA-derived nitrogen underlies obesity-related Glycine depletion. Cell Reports 33(6):108375.

[41] Martínez-Reyes, I., Chandel, N.S., 2020. Mitochondrial TCA cycle metabolites control physiology and disease. Nature Communications 11(1):102.

[42] Owen, O.E., Kalhan, S.C., Hanson, R.W., 2002. The key role of anaplerosis and cataplerosis for citric acid cycle function. Journal of Biological Chemistry 277(34):30409—30412.

[43] Keshet, R., Szlosarek, P., Carracedo, A., Erez, A., 2018. Rewiring urea cycle metabolism in cancer to support anabolism. Nature Reviews Cancer 18(10):634—645.

